Quantum beating in Rb at 18.3 THz (608 cm^{-1}) detected by parametric six-wave mixing and sum-frequency generation in $LiIO_3$

C.-J. Zhu,* Y. Xiao, A. A. Senin,† J. Gao, and J. G. Eden
Laboratory for Optical Physics and Engineering, Department of Electrical and Computer Engineering, University of Illinois, Urbana, Illinois 61801, USA

T. S. Varzhapetyan and D. H. Sarkisyan
Institute for Physical Research, Armenian Academy of Science, Ashtarak-2, 378410, Armenia
(Received 2 January 2007; published 8 May 2007)

Axially phase-matched parametric six-wave mixing (PSWM) has been observed in Rb vapor by two-photon excitation of the atom ($5s \rightarrow \rightarrow 7s, 5d$) with ~150 fs pulses, centered at $\lambda \sim 769$ nm and generated by a $Ti:Al_2O_3$ laser system. For a peak laser pulse intensity of 30 GW cm^{-2}, PSWM is observed for Rb number densities ($[Rb] > 2.5 \times 10^{15}$ cm^{-3} whereas, for $[Rb] = 2.2 \times 10^{16}$ cm^{-3}, the PSWM process is detectable for pump intensities above ~3 GW cm^{-2}. Upconversion of the 1.367 μm and 1.323 μm signal waves into the visible ($\lambda \sim 494$ nm) has been accomplished by sum frequency generation in $LiIO_3$, and quantum beating in Rb at 18.3 THz (~608 cm^{-1}) has been observed by monitoring the upconverted signal wave intensity produced in pump-probe experiments. These results broaden the scope of the wave packet detection scheme reported by Tran *et al.* [Opt. Lett. **23**, 70 (1998)] in that a variety of coherent nonlinear optical processes ($\chi^{(3)}, \chi^{(5)}, \ldots$) appear to be suitable for observing the amplitude and phase of atomic (or molecular) wave packets.

DOI: 10.1103/PhysRevA.75.053405 PACS number(s): 42.50.Md, 42.65.Ky, 42.65.Sf

I. INTRODUCTION

In 1998, Tran *et al.* [1] demonstrated that the dynamics of an atomic wave packet could be monitored by parametric four-wave mixing (PFWM) in pump-probe experiments on the femtosecond time scale. Specifically, the interference between the coherent superpositions of the Rb 7*s* and 5*d* states produced by both the pump and probe pulses (each of which produces 7*s*-5*d* quantum beating) is superimposed onto the intensity of the coherent signal wave generated at $\lambda \sim 420$ nm by the PFWM process. The frequency composition of the wave packet, reflected by the phase and amplitude of the 7*s*-5*d* quantum beating, is recovered in the macroscopic domain by Fourier analysis of the variation of the signal intensity with the pump-probe delay time (Δt). PFWM is, therefore, the means by which the temporal history of an atomic (or molecular) wave packet is coupled to a beam of coherent visible or infrared radiation. Recent experiments [2] have shown that this unique tool is capable of determining the excited state distribution of the atomic fragments produced in the dissociation of a diatomic molecule.

This paper reports the detection of quantum beating in Rb by axially phase-matched parametric *six*-wave mixing (PSWM) in which the signal waves at 1.323 and 1.367 μm (associated with the $6\,^2S_{1/2} \rightarrow 5\,^2P_{1/2,3/2}$ transitions) are upconverted to the visible by sum frequency generation (SFG) in $LiIO_3$. PSWM has not been reported previously for Rb and is characterized here for ~150 fs pump-probe laser pulses. Perhaps the greater significance of these results, however, is the confirmation they provide to the generality of the wave-packet detection scheme of Ref. [1]. In particular, the demonstration that $\chi^{(3)}$ and $\chi^{(5)}$ processes are capable of optically detecting wave packets suggests that other coherent nonlinear optical processes, resonantly enhanced by an atomic or molecular state contributing to the structure of a wave packet, are suitable as well.

Parametric four-wave mixing in the alkali vapors was first reported by Lumpkin *et al.* [3,4] in 1967 and was characterized extensively by Sorokin, Lankard, and Wynn [5,6] in the early 1970s. Its $\chi^{(5)}$ counterpart—parametric six-wave mixing—was, however, not observed for another decade. Zhang *et al.* [7] described in 1984 the generation of 23 lines attributed to PSWM in potassium vapor and, subsequently, further experiments were conducted in K (Refs. [8,9]), Na (Refs. [10,11]) and Li (Ref. [12]). Virtually all previous experimental studies of PSWM involved excitation of two photon resonant transitions of the atom with a tunable laser, pulsed on the nanosecond time scale. Figure 1 is a partial energy level diagram for atomic Rb illustrating the difference-frequency, six-wave mixing process $\omega_{S_2} = 2\omega_L - \omega_{S_1} - \omega_{S_3} - \omega_{i_{1,2}}$, where $\hbar\omega_L$ is the pump-probe laser photon energy and ω_{S_1}, ω_{S_2}, ω_{S_3}, and $\omega_{i_{1,2}}$ are the frequencies of the signal waves and idlers. Two variants of the PSWM process are illustrated in Fig. 1. One of these, discussed by Clark *et al.* [8], is a special case of the general process cited above in which $\omega_{S_3} = \omega_L$ and thus one photon is returned to the pump optical field. The distinction between the two is essentially lost in the present experiments in which the pump (and probe) laser bandwidth is ~18 nm.

We generate atomic wave packets comprising predominantly the $7\,^2S_{1/2}$ and $5\,^2D_{5/2}$ states of Rb (hereafter denoted 7*s* and $5d_{5/2}$) by exciting the resonantly enhanced, two photon $5s \rightarrow \rightarrow 7s, 5d_{5/2}$ transitions with two identical ~150 fs optical pulses, one of which (probe) is delayed in time with

*Department of Physics, School of Science, Xi'an Polytechnic University, Xi'an 710048, China.
†VLOC, Subsidiary of II-VI Inc., YAG Business Unit, 6716 Industrial Ave., Port Richey, FL 34668.

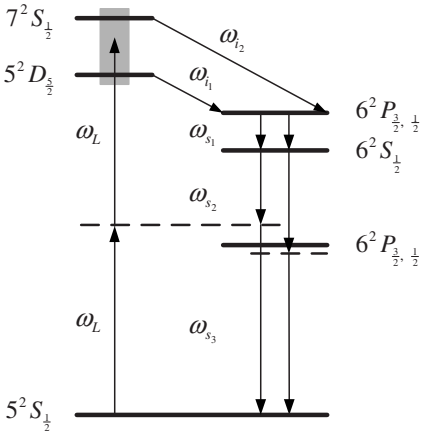

FIG. 1. Partial energy level diagram for Rb illustrating the PSWM process initiated by exciting the $5\,^2S_{1/2} \rightarrow\rightarrow 7\,^2S_{1/2}, 5\,^2D_{5/2}$ two photon transitions with ~150 fs laser pulses having a central wavelength of ~769 nm. Coherent signal waves at $\lambda_{S_1} \simeq 2.76$ μm, $\lambda_{S_2} \simeq 1323$ nm, 1367 nm, and $\lambda_{S_3} \simeq 781$, 793 nm are generated. A special case of the general PSWM process: $\omega_{S_3} = 2\omega_L - \omega_i - \omega_{S_1} - \omega_{S_2}$, in which $\omega_{S_3} = \omega_L$, is also depicted. The shaded region indicates that the bandwidth of the pump and probe laser pulses is sufficient to encompass both the $5s \rightarrow\rightarrow 7s$ and $5s \rightarrow\rightarrow 5d_{5/2}$ transitions.

respect to the other (pump) by Δt. Interference between the $7s$-$5d$ coherent superpositions produced by the pump and probe pulses, each of which produces quantum beating at 607.94 cm^{-1} (the $7s$-$5d_{5/2}$ energy defect), is detectable by observing the relative intensity of the signal or idler waves as Δt is scanned. In the PSWM process of Fig. 1, the signal wave denoted ω_{S_3} (associated with the $5p_{1/2,3/2} \rightarrow 5s$ transitions) is generated at 781and 793 nm, wavelengths that pose difficulties for reliable measurements because of their proximity to the pump and probe. Accordingly, these experiments focus on the ω_{S_2} signal waves which lie in the near-infrared (1.323 μm, 1.367 μm) and are upconverted into the visible by sum frequency generation.

II. EXPERIMENTAL ARRANGEMENT AND EMISSION SPECTRA

A schematic diagram of the experiment is shown in Fig. 2. Laser pulses, linearly polarized with a nominal temporal width of 150 fs and a central wavelength of 769 nm, are produced at a repetition frequency of 1 kHz by a $Ti:Al_2O_3$ oscillator-amplifier system. After spectrally broadening the pulses by self-phase modulation in air to a bandwidth of ~18 nm, a Michelson interferometer generates pairs of pulses, separated by an adjustable time delay (Δt). Both pulses are focused into a sapphire cell containing Rb vapor and, since the PSWM process is axially phase matched, the collinear signal waves at 1.323 and 1.367 μm are summed with the remaining pump energy (or with the copropagating signal radiation at 781 and 793 nm) in a 3-mm-thick $LiIO_3$ crystal to generate a readily detectable signal in the blue-green region of the visible spectrum. The phase-matching angle for this SFG process is ~32° with respect to the c axis

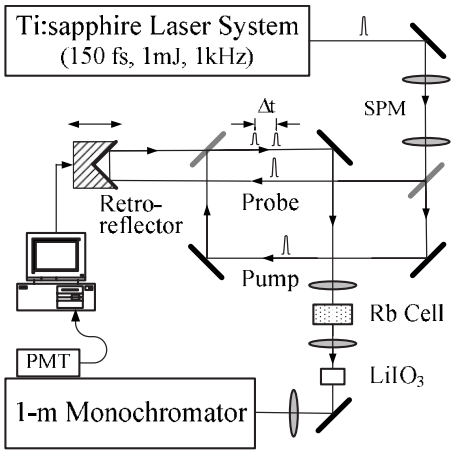

FIG. 2. Schematic diagram of the experimental arrangement. The acronyms SPM and PMT denote self-phase modulation and photomultiplier, respectively, and the thickness of the $LiIO_3$ crystal is 3 mm.

of the crystal [13] A spectrum of the forward propagating radiation in the 350–810 nm region, recorded with a 1 m spectrograph in first order for an Rb number density of $[Rb] = 2.2 \times 10^{16}$ cm^{-3}, is presented in Fig. 3. Aside from the transmitted pump/probe radiation itself, strong emission appearing at $\lambda_S \sim 420$ nm is generated by the well-known PFWM process: $\omega_S = 2\omega_L - \omega_i$, where the subscripts L, S, and i denote laser (pump), signal, and idler photons, respectively [1,2]. Upconversion of the 1.323 μm PSWM signal into the blue-green is evidenced by the peak at $\lambda \sim 494$ nm. Dominance of the 1.323 μm signal wave in the sum-frequency spectrum suggests a propensity of PSWM in Rb for the $5s \rightarrow\rightarrow 7s$, $5d_{5/2} \rightarrow 6p_{3/2} \rightarrow 6s \rightarrow 5p_{1/2} \rightarrow 5s$ process, owing to the magnitudes of the matrix elements contributing to $\chi^{(5)}$.

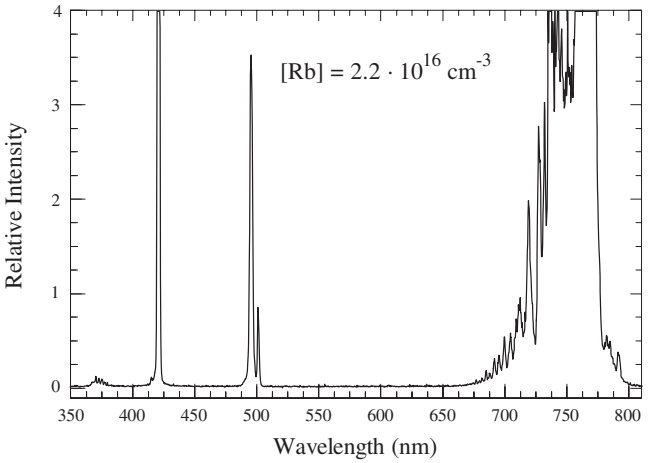

FIG. 3. Representative spectrum in the forward direction, recorded in the 350–810 nm wavelength interval for $[Rb] = 2.2 \times 10^{16}$ cm^{-3}. The peak at ~494 nm is the result of summing the residual pump with the 1.323 μm signal wave, whereas the weaker feature at ~501 nm is the sum of the PSWM signal waves at 1.367 μm and 793 nm. Molecular emission from the Rb dimer is also evident ($\lambda \sim 370$ nm, and 675–750 nm).

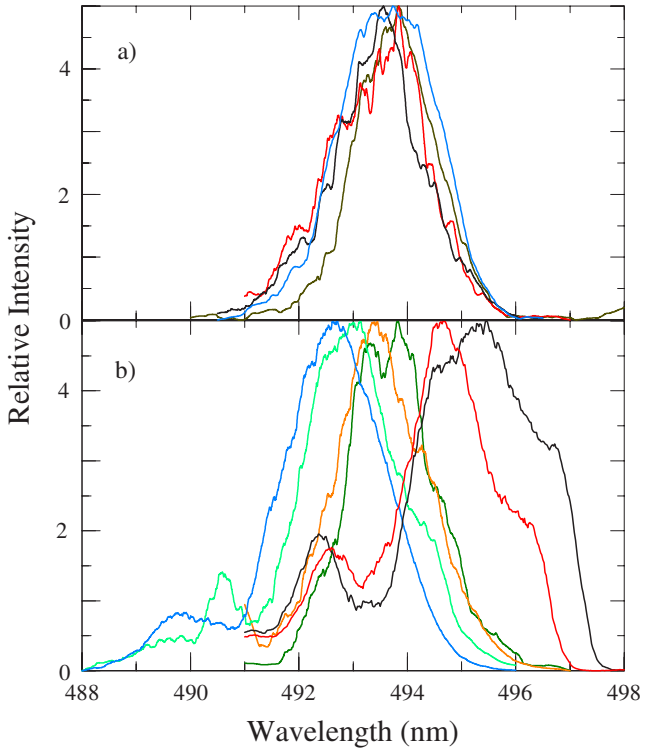

FIG. 4. (Color) Magnified and normalized spectra for the SFG of the residual pump with the 1.323 μm PSWM signal: (a) several superimposed spectra acquired for a fixed orientation of the $LiIO_3$ crystal; (b) representative spectra observed when rotating the crystal.

The weaker feature in Fig. 3 at ~501 nm appears to be the result of summing 1.367 μm and 793 nm signal photons in the $LiIO_3$ crystal in a collinear geometry. Molecular emission from the homonuclear Rb_2 is also evident in the near-ultraviolet (~370 nm) and near-infrared (675–750 nm). Neither the 420 nm PFWM nor ~494 nm PSWM signals are detectable in the backward direction. Also, owing to the bandwidth of the pump, the SFG signal can be tuned from ~492 to ~496 nm by rotating the $LiIO_3$ crystal. Panel (a) of Fig. 4 illustrates the reproducibility of the (normalized) SFG spectra observed for a fixed orientation of the $LiIO_3$ crystal and the Rb number density held constant. Several representative spectra recorded while rotating the crystal are illustrated in the lower half of Fig. 4.

It should be emphasized that both the 1.323 and 1.367 μm signals have been observed directly with a spectrometer-CCD detection system that is sensitive in the near infrared to wavelengths beyond 1.5 μm. However, upconverting the PSWM signal into the visible by SFG offers two distinct incentives when conducting and interpreting the experiments reported here. The first of these is the superior performance of visible photodetectors with respect to dynamic range and sensitivity. Of greater import, however, is the fact that the generation of the blue-green radiation is itself instructive. Specifically, Figs. 3 and 4 demonstrate clearly that the six-wave mixing process observed in these experiments is truly parametric in that the residual pump and the signal wave are present simultaneously in the $LiIO_3$ crystal. This result, axial phase-matched PSWM, contrasts with the noncollinear geometry of Lvovsky *et al.* [14] who showed convincingly that, when excited by 4 ps laser pulses, the $5s \rightarrow \rightarrow 5d \rightarrow 6p \rightarrow 5s$ PFWM process is time delayed (i.e., the idler and signal are produced following the termination of the driving optical field). The idler is generated by superfluorescence but the overall process is, nevertheless, coherent.

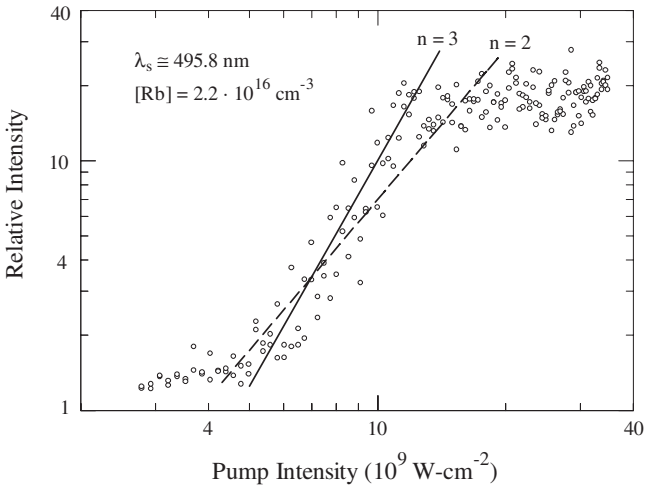

FIG. 5. Variation of the upconverted signal intensity (at $\lambda \simeq 496$ nm) with the pump laser intensity for a Rb number density ([Rb]) of 2.2×10^{16} cm^{-3}. The lines illustrate an I_p^n dependence for the blue-green intensity where $n=2$ and 3 for the dashed and solid lines, respectively.

III. RESULTS AND DISCUSSION

Further insight into the dominant processes occurring in these experiments is provided by examining the variation of the signal wave intensity with that of the pump. Measurements of the dependence of the relative, upconverted signal intensity ($\lambda \sim 496$ nm) on the pump intensity I_p for $3 \lesssim I \lesssim 35$ GW cm^{-2} and the Rb number density [Rb] held constant at 2.2×10^{16} cm^{-3} are summarized in Fig. 5. The solid and dashed lines in the figure indicate a variation of the blue-green intensity with I_p of I_p^n, where n is an integer. It is evident that, for $I_p \gtrsim 5$ GW cm^{-2}, the upconverted signal wave intensity (I_S) rises rapidly and, as depicted by the solid line, exhibits a cubic dependence on I_p over a limited range in pump intensity. For comparison, the dashed line in Fig. 5 displays a quadratic variation of I_S with the pump intensity. Above $I_p \sim 10$ GW cm^{-2}, the blue-green intensity saturates and rises slowly up to the highest values of I_p investigated (~35 GW cm^{-2}). The cubic dependence of the upconverted signal wave intensity on I_p is precisely the expected behavior for the PSWM processes discussed by Wang and coworkers[10] for Na, and Chen *et al.* [12] for Li. One scenario discussed in Ref. [12] is that in which three photons are absorbed from the pump field (not illustrated in Fig. 1) and a hyper-Raman scattering process populates the 6*s* state of Rb. An alternative mechanism is that shown in Fig. 1 (and discussed previously) in which two photon excitation of the Rb

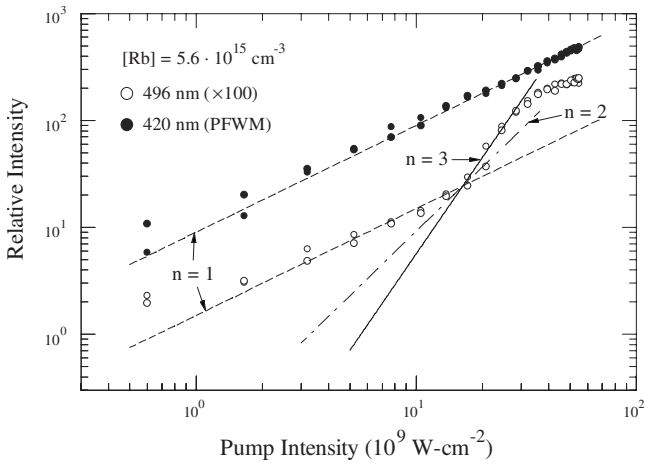

FIG. 6. Comparison of the dependence of the PSWM 496 nm intensity on I_p, with that for the 420 nm signal wave generated by PFWM. The PFWM data are indicated by the solid circles (●) whereas the PSWM results are represented by the open circles (○). The dashed lines illustrate a linear dependence on pump intensity (I_p) and the broken (— -) and solid lines represent the functional form I_p^n for $n=2$ or 3, respectively.

$(7s,5d_{5/2})$ states is followed by the participation of a third pump photon to complete the PSWM process.

A comparison of the relative intensities in the violet (420 nm) and blue-green (496 nm), generated by PFWM and PSWM, respectively, is presented in Fig. 6 for [Rb] fixed at 5.6×10^{15} cm^{-3}, a value lower than that of Fig. 5 by a factor of ~4, and $0.6\leqslant I_p\leqslant 55$ GW cm^{-2}. For clarity, the magnitude of the PSWM data has been scaled by a factor of 100. Notice that, in this range of pump intensity, the PFWM signal intensity has saturated as evidenced by the linear dependence of the 420 nm intensity on I_p. The cubic variation of I_{496} with I_p is once again apparent over a restricted range in pump intensity but the reduced value of [Rb] (relative to Fig. 5) has the effect of increasing the magnitude of the pump intensity at which this rapid increase in blue-green intensity is observed. Specifically, the onset of the I_p^3 dependence is observed for $I_p\sim20$ GW cm^{-2}, or approximately a factor of 4 higher than the pump intensity threshold of Fig. 5. This result is consistent with the expected linear dependence of $\chi^{(5)}$ on [Rb] (see, for example, Refs. [7,9]) and the factor of 4 difference in Rb density between Figs. 5 and 6. It should also be mentioned that we were unable to detect the 492–496 nm upconverted signal for $[\mathrm{Rb}]\leqslant2.5\times10^{15}$ cm^{-3} when $I_p=30$ GW cm^{-2}, whereas the PFWM signal wave was observed at Rb number densities two orders of magnitude lower ($[\mathrm{Rb}]\geqslant3\times10^{13}$ cm^{-3}).

Further experiments were conducted to investigate the feasibility of detecting atomic wave packets in Rb by monitoring the intensity of the upconverted PSWM signal wave. Toward that end, two identical pulses were (as illustrated in Fig. 1) produced by a beam splitter and one (the probe pulse) was time delayed by Δt with respect to the other (pump pulse) by a computer-controlled Michelson interferometer. Figure 7 is a representative scan for $0\leqslant\Delta t\leqslant45$ ps of the relative 494 nm PSWM intensity, and the inset to the figure shows the Fourier domain representation (FFT) of the scan.

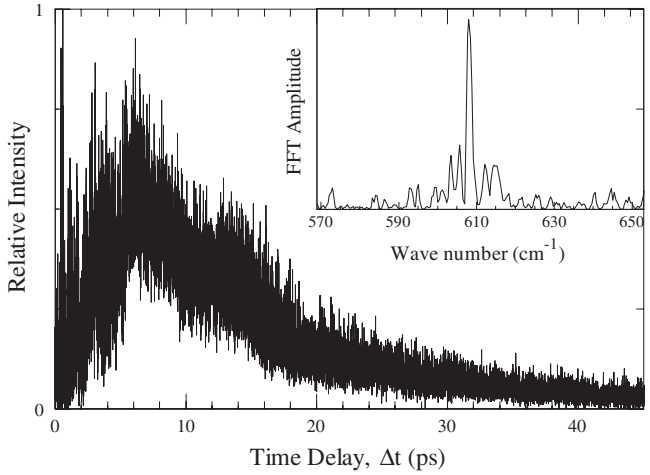

FIG. 7. Dependence of the relative 494 nm intensity on the time delay Δt for $[\mathrm{Rb}]=1.1\times10^{16}$ cm^{-3} and $0\leqslant\Delta t\leqslant45$ ps. The inset is an FFT of the scan, showing a distinct peak at the $7s$-$5d_{5/2}$ quantum beating frequency of ~608 cm^{-1} (18.3 THz).

The dominant feature in the Fourier spectrum, lying at ~608 cm^{-1}, is the result of quantum beating between the $7s$ and $5d_{5/2}$ states of the atom ($7s$-$5d_{5/2}$ energy defect is 607.94 cm^{-1}). On either side of the strong peak are sets of at least two sidebands that have been shown recently [15] to arise from interactions (primarily dipole-dipole interactions) between excited atoms at long range. The comparatively low signal-to-noise (S/N) ratio for the spectrum of the inset to Fig. 7 is the result of two factors, one of which is the dc component of the background noise originating from the pump laser pulse during the PSWM process, noise that is superimposed onto the 494 nm radiation through sum frequency generation (SFG). Another factor limiting the resolution and peak contrast in the inset of Fig. 7 is that the spectral and angular bandwidth for the SFG process has not been optimized. Since the spectral phase-matching bandwidth for a $LiIO_3$ crystal 1 cm in length is only ~6 cm^{-1}, reducing the thickness of the crystal in these experiments from its present value of 3 mm to ~100 μm will undoubtedly improve the S/N ratio of the Δt scan of Fig. 7 and reduce distortion in its associated Fourier spectrum. Despite these considerations, the sidebands and central peak at 608 cm^{-1} observed in the frequency domain confirm that Rb ($7s-5d_{5/2}$) quantum beating has been detected by PSWM.

IV. SUMMARY AND CONCLUSIONS

Quantum beating between the $7s$ and $5d_{5/2}$ states of Rb has been observed by PSWM on the femtosecond time scale. The upconversion of the signal waves at 1.323 and 1.367 μm into the visible and the clear presence of a dominant peak at 608 cm^{-1} in the Fourier domain, demonstrate that the entire PSWM process is coherent and that atomic (or molecular) wave packets can be monitored by a $\chi^{(5)}$ process. The observation that both FWM and PSWM are capable of detecting wave packets suggests that the concept of monitoring atomic or molecular wave packets by a nonlinear coherent process is

broad and, specifically, that other nonlinear processes, such as third harmonic generation, will also prove to be successful. Measurements of the dependence of the signal wave intensity on the pump pulse intensity exhibit a threshold for the PSWM process of $\sim$1–5 GW cm^{-2}, depending upon the Rb ground state number density. Since the Fourier spectrum of the wave packet's temporal history is prescribed by eigenstates of the atom (or molecule), the application of this detection scheme as a local oscillator in spectroscopy, as well as for the detailed examination of molecular fragmentation or atomic dipole-dipole interactions, appear to be promising.

ACKNOWLEDGMENT

The support of this work by the U.S. Air Force Office of Scientific Research (H. R. Schlossberg) under Grant No. F49620-03-1-0391 is gratefully acknowledged.

[1] H. C. Tran, P. C. John, J. Gao, and J. G. Eden, Opt. Lett. **23**, 70 (1998).
[2] A. A. Senin, H. C. Tran, J. Gao, Z.-H. Lu, C.-J. Zhu, A. L. Oldenburg, J. R. Allen, and J. G. Eden, Chem. Phys. Lett. **381**, 53 (2003).
[3] O. J. Lumpkin, P. P. Sorokin, and J. R. Lankard, Bull. Am. Phys. Soc. **12**, 1054 (1967).
[4] O. J. Lumpkin, Jr., IEEE J. Quantum Electron. **QE-4**, 226 (1968).
[5] P. P. Sorokin and J. R. Lankard, IEEE J. Quantum Electron. **9**, 227 (1973).
[6] P. P. Sorokin, J. J. Wynne, and J. R. Lankard, Appl. Phys. Lett. **22**, 342 (1973).
[7] P.-L. Zhang, Y.-C. Wang, and A. L. Schawlow, J. Opt. Soc. Am. B **1**, 9 (1984).
[8] B. K. Clark, M. Masters, and J. Huennekens, Appl. Phys. B: Photophys. Laser Chem. **47**, 159 (1988).
[9] Z. J. Jabbour, M. S. Malcuit, and J. Huennekens, Appl. Phys. B: Photophys. Laser Chem. **52**, 281 (1991).
[10] Z. G. Wang, H. Schmidt, and B. Wellegehausen, Appl. Phys. B: Photophys. Laser Chem. **44**, 41 (1987).
[11] M. A. Moore, W. R. Garrett, and M. G. Payne, Phys. Rev. A **39**, 3692 (1989).
[12] F. Z. Chen, X. F. Han, and C. Y. R. Wu, Appl. Phys. B: Photophys. Laser Chem. **56**, 113 (1993).
[13] V. G. Dmitriev, G. G. Gurzadyan, and D. N. Nikogosyan, *Handbook of Nonlinear Optical Crystals*, Springer Series in Optical Sciences, Vol. 64, 3rd ed. (Springer-Verlag, Berlin, 1999).
[14] A. I. Lvovsky, S. R. Hartmann, and F. Moshary, Phys. Rev. Lett. **82**, 4420 (1999).
[15] F. Shen, J. Gao, A. A. Senin, C. J. Zhu, J. R. Allen, Z. H. Lu, Y. Xiao, and J. G. Eden (unpublished).